Evidence for quark-hadron duality in γ^{*}p helicity cross sections

S. P. Malace, W. Melnitchouk, and A. Psaker

Phys. Rev. C **83**, 035203 — Published 29 March 2011

DOI: 10.1103/PhysRevC.83.035203

Evidence for quark-hadron duality in $\gamma^* p$ helicity cross sections

S. P. Malace[1], W. Melnitchouk[2] and A. Psaker[3]

[1] *Department of Physics, Duke University, Durham, North Carolina 27708, USA*

[2] *Jefferson Lab, Newport News, Virginia 23606, USA*

[3] *American University of Nigeria, Yola, Nigeria*

Abstract

Combining data on unpolarized and polarized inclusive proton structure functions, we perform the first detailed study of quark-hadron duality in individual helicity-1/2 and 3/2 virtual photoproduction cross sections. We find that duality is realized more clearly in the helicity-1/2 channel, with duality violating corrections $\lesssim 10\%$ over the entire nucleon resonance region, while larger, $\lesssim 20\%$ corrections are found in the helicity-3/2 sector. The results are in general agreement with quark model expectations, and suggest that data above the Δ resonance region may be used to constrain both spin-averaged and spin-dependent parton distributions.

I. INTRODUCTION

The duality between quark and hadron descriptions of physical observables reveals a fascinating connection between the physics of quark confinement at low momentum scales and asymptotic freedom at large momenta. The striking manifestation of this duality in inclusive electron–nucleon scattering, first observed [1] even before the advent of QCD, has motivated considerable effort in recent years to explore this phenomenon empirically, as well as to understand its origins theoretically (for a review see Ref. [2]).

From a practical perspective, the quantitative demonstration of the similarity between the structure functions measured in the nucleon resonance region and those in the deep inelastic continuum, at higher energies, opens up the intriguing possibility of using resonance region data to provide constraints on leading twist parton distribution functions (PDFs). Attempts to utilize this connection have begun to be explored in recent global PDF fits [3] (see also Ref. [4]), where data on the unpolarized proton and deuteron F_2 structure functions at final state hadronic masses W as low as ~ 1.7 GeV have been used to extend determinations of PDFs to larger values of the Bjorken scaling variable $x = Q^2/2M\nu$, where Q^2 and ν are the four-momentum squared and energy transferred to the proton, and M is the proton mass.

The availability of high-luminosity electron beams at Jefferson Lab has enabled high-precision measurements of various structure functions to be made over the past decade. These data have now firmly established the existence of duality in the proton F_2 and F_L structure functions [5–8], and have provided tantalizing glimpses of its spin and flavor dependence in polarized [9, 10] and semi-inclusive scattering measurements [11]. Recently a new method [12] was used to extract also the neutron F_2 structure function from inclusive proton and deuterium data in the nucleon resonance region [13], leading to the first quantitative determination of duality in the neutron's unpolarized structure functions. This observation suggested that duality is indeed a general feature of the resonance-scaling transition, and not due to accidental cancellations of quark charges [14].

Because of the considerably larger data base of spin-averaged cross sections than polarization asymmetries, duality in the spin-dependent g_1 and g_2 structure functions has not yet been established to the same precision as for the unpolarized $F_{1,2}$ structure functions. An additional complication arises from the fact that for spin-dependent quantities one deals with differences of cross sections, which are not restricted to be positive. For example, in

the Δ resonance region the g_1 structure function of the proton, especially at low Q^2, is large and negative, while for the same x and higher Q^2 (hence higher $W^2 = M^2 + Q^2(1-x)/x$) the structure function measured in the deep inelastic region is positive. Such strong violation of duality would limit the use of resonance region data to constrain spin-dependent PDFs. Furthermore, the neutron g_1 structure function changes sign as a function of x, so cannot be used to study ratios of resonance to deep inelastic structure functions or the relative size of duality violations.

On the other hand, duality violation may be less severe, even at low W, in individual virtual photoabsorption helicity cross sections, defined by projecting the total spin of the virtual photon–proton center of mass system along the photon direction. The helicity-1/2 projection, $\sigma_{1/2}$, represents the cross section for equal initial and excited hadronic state helicities, while the helicity-3/2 projection, $\sigma_{3/2}$, involves a change of the hadron helicities by two units. The sums and differences of the helicity cross sections, which are positive definite, correspond to the unpolarized and spin polarized structure functions, respectively.

At high Q^2 and W^2 the helicity cross sections are proportional to the positive and negative helicity PDFs, $q^{\pm}(x, Q^2)$, which describe the distribution of quarks with spin parallel or antiparallel to that of the nucleon. As with the cross sections, the helicity PDFs are defined to be positive, and in a way represent more fundamental objects than the spin-averaged and spin-dependent PDFs. In fact, from perturbative QCD arguments one can make definite predictions for the behavior of the helicity PDFs in the limit $x \to 1$, with $q^-/q^+ \sim (1-x)^2$ [15, 16]. These predictions can be tested by studying the asymptotic x dependence of helicity cross sections, which is difficult, however, because of the rapidly decreasing rates as $x \to 1$. Indeed, since large x generally corresponds to low W, determining the large-x behavior of inclusive cross sections at any finite Q^2 will necessarily involve the resonance region.

In this paper we perform the first detailed study of quark-hadron duality in $\gamma^* p$ helicity cross sections, by combining previously measured sets of data on inclusive spin-averaged cross sections and double polarization asymmetries from Jefferson Lab and elsewhere. These data are used to quantify the degree of duality violation in each of the three prominent nucleon resonance regions, as well as over the entire range $W < 2$ GeV.

In Sec. II we begin by defining the relevant cross sections and distributions used in this analysis. Section III outlines the data analysis, describing the construction of the helicity cross sections form separate measurements of spin-averaged and spin-dependent structure

functions. Results of the analysis are presented in Sec. IV, for the x dependence of helicity structure functions in several fixed-Q^2 bins ranging from $Q^2 = 1.7$ to 5 GeV^2, as well as for integrals over the various resonance regions. Comparison of the resonance data with parametrizations of data at higher energies then allow the first determination of the extent to which duality holds in helicity cross sections over this range. We also compare our findings with quark models that predict specific patterns of duality violation in structure functions. Finally, in Sec. V we draw some conclusions from this analysis and outline its broader implications for our understanding of quark-hadron duality as well as its practical exploitation.

II. HELICITY STRUCTURE FUNCTIONS

The differential cross section for the inclusive scattering of a longitudinally polarized electron with helicity $h = \pm 1$ from a proton with polarization P_z along the virtual photon direction can be written as

$$\frac{d\sigma}{d\Omega dE'} \;=\; \Gamma\left(\sigma_T + \varepsilon\sigma_L + hP_z\sqrt{1-\varepsilon^2}\sigma'_{TT}\right), \tag{1}$$

where E' is the scattered electron energy, Γ is the flux of virtual photons and ε is the transverse photon polarization [17]. The photoabsorption cross sections for transversely polarized virtual photons are related to the helicity cross sections $\sigma_{1/2}$ and $\sigma_{3/2}$ by

$$\sigma_T \;=\; \frac{1}{2}\left(\sigma_{1/2} + \sigma_{3/2}\right), \tag{2}$$

$$\sigma'_{TT} \;=\; \frac{1}{2}\left(\sigma_{3/2} - \sigma_{1/2}\right), \tag{3}$$

while the cross section for longitudinally polarized photons is given by the longitudinal structure function. The cross section $\sigma_{1/2}$ ($\sigma_{3/2}$) corresponds to the spins of the virtual photon and proton antialigned (aligned) in the center of mass system, so that the helicity of the excited nucleon state after absorbing a photon is $+1/2$ ($+3/2$). Whereas the $\sigma_{1/2}$ cross section conserves the nucleon helicity, the $\sigma_{3/2}$ changes the nucleon helicity by two units.

For convenience we define dimensionless helicity structure functions $H_{1/2}$ and $H_{3/2}$ in terms of the cross sections by

$$H_{1/2} \;=\; \frac{MK}{4\pi^2\alpha}\,\sigma_{1/2}, \qquad H_{3/2} \;=\; \frac{MK}{4\pi^2\alpha}\,\sigma_{3/2}, \tag{4}$$

where $\alpha = e^2/4\pi$ and $K = (W^2 - M^2)/2M$ is associated with the choice of the virtual photon flux in the Hand convention [18]. The helicity structure functions can then be written in terms of the usual unpolarized F_1 and polarized $g_{1,2}$ structure functions as

$$H_{1/2} = F_1 + g_1 - \frac{Q^2}{\nu^2} g_2, \tag{5a}$$

$$H_{3/2} = F_1 - g_1 + \frac{Q^2}{\nu^2} g_2, \tag{5b}$$

each of which is a function of two variables, typically taken to be x and Q^2. In the limit where both Q^2 and W^2 are large, with x finite (Bjorken limit), the F_1 and g_1 structure functions can be written, at leading order in α_s, in terms of leading twist PDFs,

$$F_1 = \frac{1}{2} \sum_q e_q^2 \, (q + \bar{q}), \tag{6a}$$

$$g_1 = \frac{1}{2} \sum_q e_q^2 \, (\Delta q + \Delta \bar{q}), \tag{6b}$$

where $q = q^+ + q^-$ and $\Delta q = q^+ - q^-$ are the spin-averaged and spin-dependent PDFs. In this case the helicity structure functions become

$$H_{1/2} = \sum_q e_q^2 \, (q^+ + \bar{q}^+), \tag{7a}$$

$$H_{3/2} = \sum_q e_q^2 \, (q^- + \bar{q}^-), \tag{7b}$$

so that in this limit $H_{1/2}$ is determined by the q^+ PDFs while $H_{3/2}$ is determined by the q^- PDFs (the antiquark distributions $\bar{q}^+$ and $\bar{q}^-$ are suppressed by additional powers of $(1-x)$ compared with the quark PDFs). In the $x \to 1$ limit the leading behavior of the helicity distributions is predicted from perturbative QCD to be $q^+ \sim (1-x)^3$ and $q^- \sim (1-x)^5$ if the nucleon ground state wave function is dominated by its S-wave component [15, 16], or $q^- \sim (1-x)^5 \log^2(1-x)$ if one includes orbital angular momentum [19].

III. DATA ANALYSIS

The experimental $H_{1/2}$ and $H_{3/2}$ helicity structure functions used in this analysis were obtained by combining measurements of g_1/F_1 ratios from Jefferson Lab experiment EG1b (E91-023) in CLAS [20] with the unpolarized F_1 structure function from the empirical

Christy-Bosted (CB) global fit [21]. For the small correction from the g_2 structure function we use the phenomenological parametrization of Ref. [22].

The CLAS E91-023 data set represents one of the few high-precision measurements of g_1/F_1 for the proton at moderate to large x ($x > 0.15$), covering a large Q^2 range from 0.05 to 5 GeV^2, over both the resonance and DIS regions. The empirical CB global fit uses measurements of inclusive inelastic electron-proton cross sections in the kinematic range of $Q^2 < 8$ GeV^2 and W between 1.1 and 3.1 GeV. The fit is constrained by high precision longitudinal and transverse separated cross section measurements from Jefferson Lab Hall C [6], unseparated Hall C measurements up to Q^2 of 7.5 GeV^2 [8], and photoproduction data at $Q^2 = 0$. This fit was chosen because it covers a wide kinematic range and uses both transverse and longitudinal cross sections, which is particularly important for the F_1 estimation. Due to the scarcity of g_2 measurements, especially in the resonance region, we use the phenomenological parametrization of Ref. [22], which is developed for $x > 0.02$ using DIS data with Q^2 up to 50 GeV^2 as well as experimental results on both photo- and electroproduction of proton resonances.

The statistical uncertainties for $H_{1/2}$ and $H_{3/2}$ were calculated from those of the g_1/F_1 measurements [20]. The systematic uncertainties were obtained from those of g_1/F_1, F_1 and g_2 by varying these quantities within the limits given by their systematics. The resulting variations of $H_{1/2}$ and $H_{3/2}$ were then added in quadrature to obtain the total systematic uncertainty. Note that since $H_{1/2}$ and $H_{3/2}$ are different combinations of the same structure functions (differing only in relative sign, Eqs. (5)), the resulting absolute uncertainties are the same for the two cross sections. However, since $H_{3/2} \ll H_{1/2}$ the relative uncertainties will be different, with that on $H_{3/2}$ much greater than on $H_{1/2}$.

The theoretical $H_{1/2}$ and $H_{3/2}$ structure functions were obtained by combining g_1 from the Blümlein-Böttcher (BB) global parametrization [23] of spin-dependent structure functions with F_1 constructed from the F_2 global fit of Alekhin *et al.* [4] and the R1998 parametrization of the longitudinal to transverse cross section ratio R [24]. The BB global fit [23] is based on a next-to-leading order QCD analysis of the world data on polarized deep inelastic scattering, and includes possible higher twist contributions. The analysis finds that for both proton and deuteron targets the higher twist corrections to g_1 are consistent with zero, within the large uncertainties of the data. For the g_2 structure function we therefore use the Wandzura-Wilczek relation [25] with g_1 from the BB fit.

The global fit of Alekhin *et al.* [4] provides QCD parametrizations for both the F_1 and F_2 structure functions. While the F_2 fit reproduces well the available F_2 data, the F_1 fit shows some discrepancies at low W with the high-precision longitudinal and transverse separated cross section measurements from Jefferson Lab Hall C [6]. We find that a good description of the Hall C F_1 data can be obtained by using the F_2 fit from Ref. [4] with the R1998 parametrization of R.

IV. RESULTS

The results for the helicity structure functions $H_{1/2}$ and $H_{3/2}$ are shown in Figs. 1 and 2 as a function of x for several fixed Q^2 values ranging from $Q^2 = 1.7$ GeV^2 to 5 GeV^2. The data are compared with curves (labeled "theory") constructed from global fits to structure functions in the deep inelastic region at higher W, as outlined in Sec. III above. The resonance region data are in excellent agreement with the global fit for the $H_{1/2}$ structure function for the kinematics considered. The agreement for $H_{3/2}$ is also quite good overall, although here the "theory" curve slightly underestimates the data, especially at lower Q^2 and in the Δ resonance region, where a prominent peak stands out. This can be understood from the fact that at low Q^2 the Δ contribution to F_1 is positive, while that to g_1 is negative, thereby cancelling in $H_{1/2}$ but reinforcing in $H_{3/2}$.

The degree to which duality holds can be quantified by considering integrals of the structure functions over individual resonance regions, ΔW,

$$I(\Delta W, Q^2) \;=\; \int_{\Delta W} dx\, \mathcal{F}(x, Q^2), \tag{8}$$

where $\mathcal{F} = H_{1/2}, H_{3/2}, F_1$ or g_1. Following earlier data analyses [5, 8, 13], we take for Δ the three prominent resonance regions, defined on the intervals

- 1$^{\rm st}$ resonance region: $1.3 \leq W^2 \leq 1.9$ GeV^2
- 2$^{\rm nd}$ resonance region: $1.9 \leq W^2 \leq 2.5$ GeV^2
- 3$^{\rm rd}$ resonance region: $2.5 \leq W^2 \leq 3.1$ GeV^2

as well as the entire resonance region $W^2 \leq 4$ GeV^2. These are shown in Figs. 3 and 4 for the $H_{1/2}$ and $H_{3/2}$ cases, respectively, with the integrals for F_1 and g_1 shown in comparison. Because $H_{1/2}$ involves a sum of the (positive) F_1 and (generally positive) g_1 structure

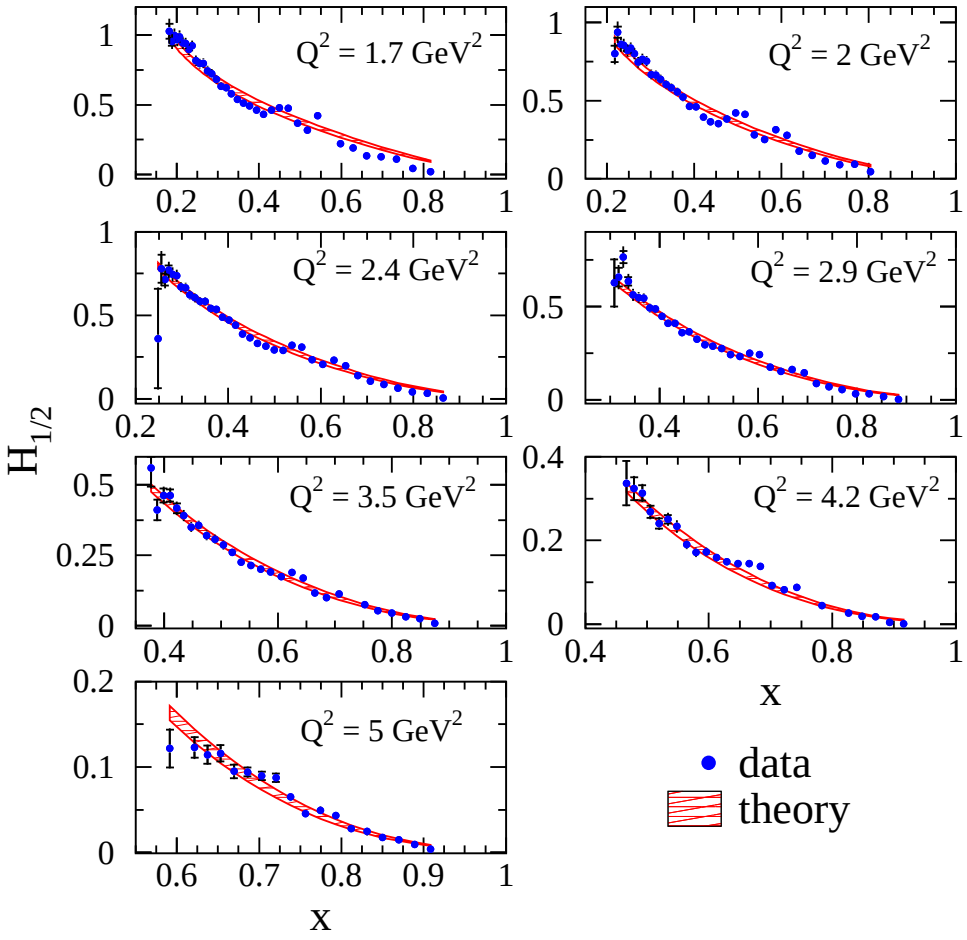

FIG. 1: Scaled helicity-1/2 cross section $H_{1/2}$ as a function of x for various Q^2 bins. The bands (labeled "theory") represent a global fit to high-W data (see text).

functions, the $H_{1/2}$ data are generally larger in magnitude than F_1 and g_1. Above the first resonance region the agreement with the global fits (shaded regions) is extremely good over the entire range of Q^2 considered for each of the $H_{1/2}$, F_1 and g_1 structure functions. The agreement in the first resonance region is markedly worse, reflecting the strong violation of duality in the g_1 structure function in the vicinity of the Δ resonance. This violation persists until $Q^2 \approx 3$ GeV^2, above which the resonance and deep inelastic data are in better agreement.

For the $H_{3/2}$ structure function, because this involves the difference between F_1 and g_1, its magnitude is considerably smaller than that of F_1. Again, duality violation is strongest

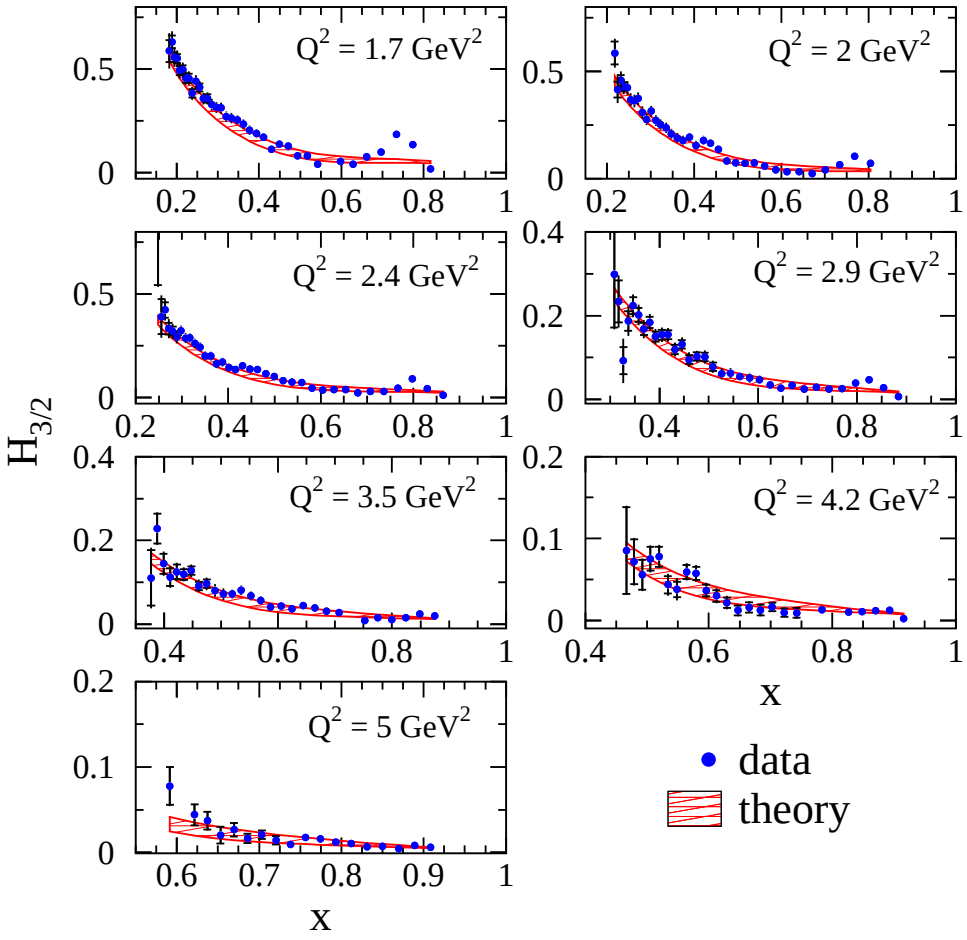

FIG. 2: As in Fig. 1 but for the helicity-3/2 cross section $H_{3/2}$.

in the Δ region, with generally good agreement between resonance and deep inelastic data at higher W. While the violations of duality are expected to diminish at larger Q^2, the decreasing magnitude of the higher-Q^2 integrals makes it more difficult to quantify the violation accurately.

To ameliorate this problem we compute the ratios of the integrals of the resonance region data to those of the global fits, shown in Fig. 5 for $H_{1/2}$ and $H_{3/2}$. In general these ratios show that duality violation is stronger in the helicity-3/2 channel than in the helicity-1/2, with the duality violating corrections for $H_{3/2}$ positive in the first resonance region and negative in the second resonance region. As could be expected, the differences between the data and theory are largest in the Δ region for both $H_{1/2}$ and $H_{3/2}$. The larger uncertainties

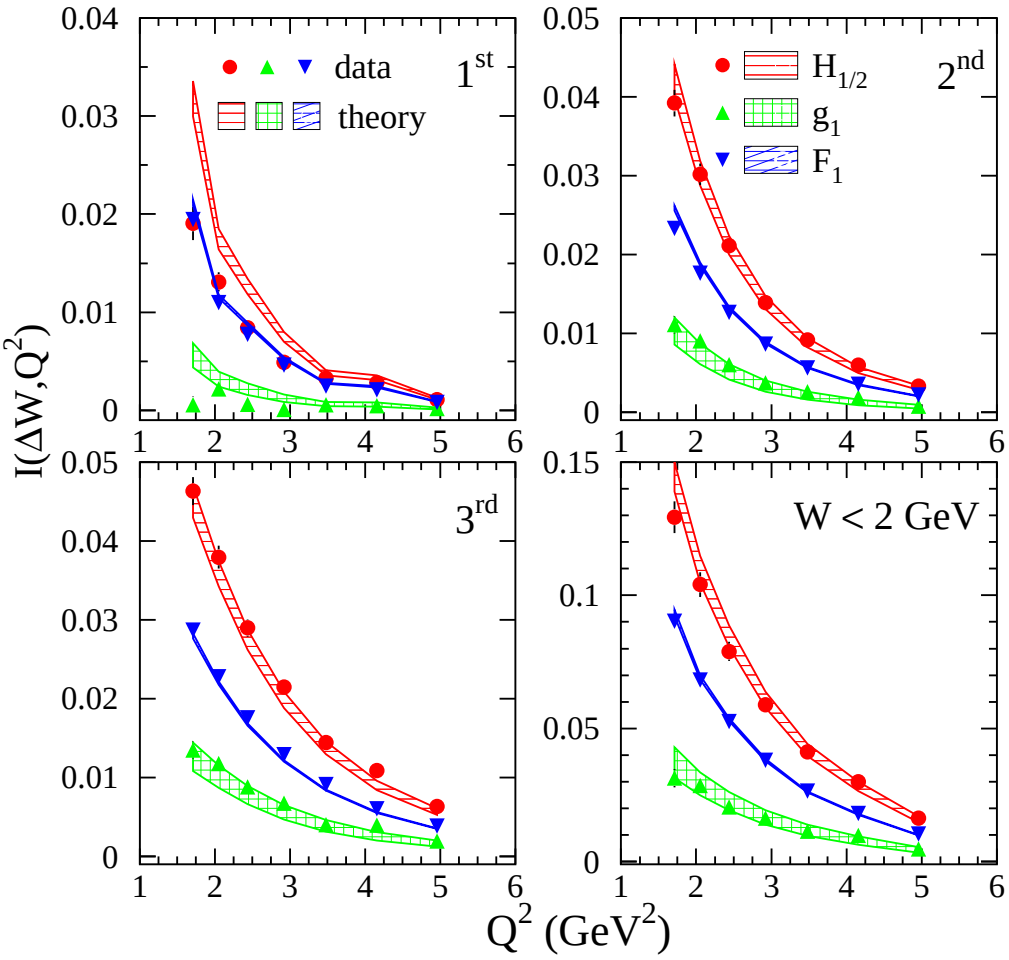

FIG. 3: Integrals $I(\Delta W, Q^2)$ of the scaled helicity-1/2 structure function $H_{1/2}$ in various resonance regions ΔW (1st, 2nd, 3rd and $W < 2$ GeV) versus Q^2. For comparison the corresponding integrals of the g_1 and F_1 structure functions are also shown. The bands represent a global fit to high-W data (see text).

on the $H_{3/2}$ data reflects the fact that $H_{3/2} \ll H_{1/2}$. Integrating over the entire $W < 2$ GeV region, the duality violation is $\lesssim 10\%$ for $H_{1/2}$ and $\lesssim 20\%$ for $H_{3/2}$ at $Q^2 \leq 4$ GeV^2. This is considerably smaller than the corresponding duality violation found in the spin-dependent g_1 structure function [9].

Our results can be compared with quark model predictions for the relative strengths of the $N \to N^*$ transitions. In Tab. 1 these are displayed for $H_{1/2}$ and $H_{3/2}$ in the various SU(6)^P = **56**$^+$ ($L = 0$) and **70**$^-$ ($L = 1$) representations [26, 27], with each representation

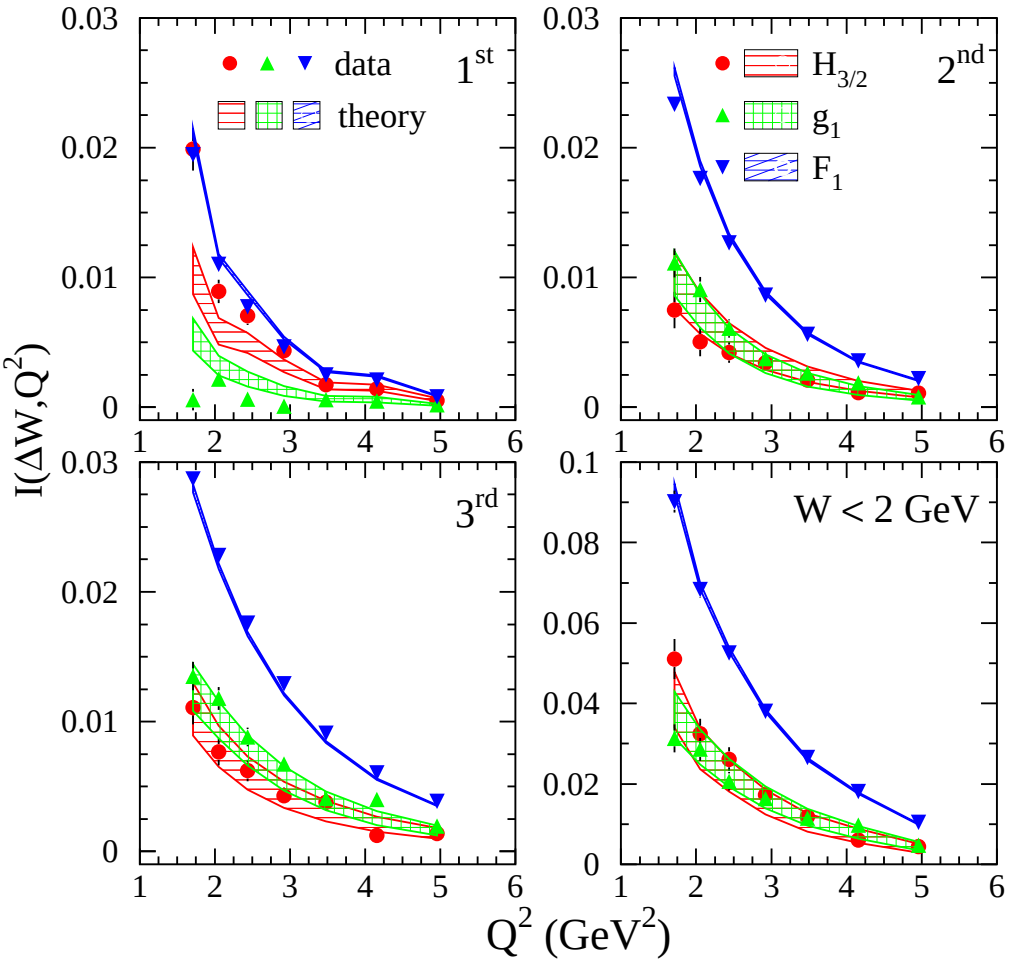

FIG. 4: As in Fig. 3 but for the helicity-3/2 structure function $H_{3/2}$.

weighted equally. The contributions from the symmetric and antisymmetric components of the ground state nucleon wave function enter with strengths λ and ρ, respectively, and the SU(6) limit corresponds to $\lambda = \rho$. The usual quark model assignments of the excited states have the nucleon and Δ in the quark spin-$\frac{1}{2}$ $^2\mathbf{8}$ and quark spin-$\frac{3}{2}$ $^4\mathbf{10}$ representations of $\mathbf{56}^+$, respectively. For the odd parity states the $^2\mathbf{8}$ multiplet contains the states $S_{11}(1535)$ and $D_{13}(1520)$, which dominate the second resonance region; the $^4\mathbf{8}$ contains the $S_{11}(1650)$, $D_{13}(1700)$ and $D_{15}(1675)$; and the isospin-$\frac{3}{2}$ states $S_{31}(1620)$ and $D_{33}(1700)$ belong to the $^2\mathbf{10}$ representation [28].

With the exception of the Δ region, the $H_{1/2}$ structure function is predicted to be much larger than the $H_{3/2}$, as is borne out by the data in Figs. 1 and 2. The relatively small

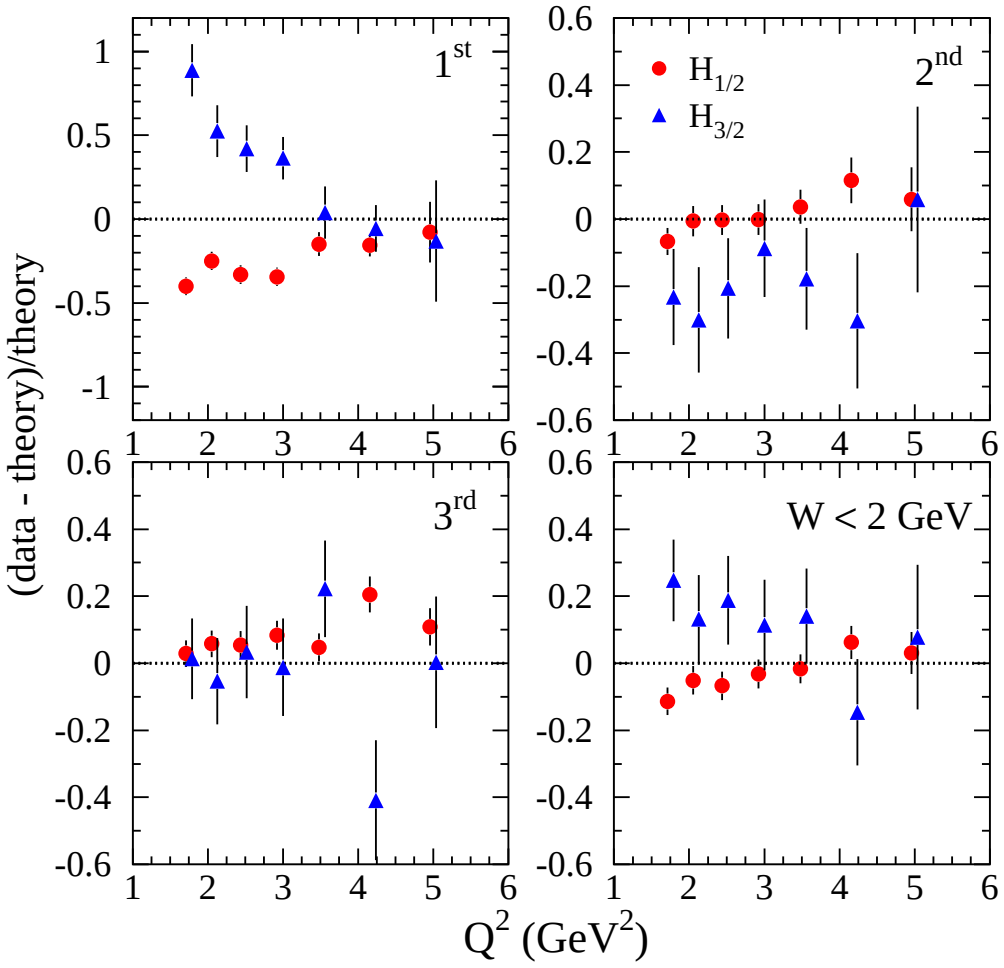

FIG. 5: Ratio (data – theory)/theory for the scaled helicity cross sections $H_{1/2}$ and $H_{3/2}$ in various resonance regions ΔW (1st, 2nd, 3rd and $W < 2$ GeV) versus Q^2. Some of the points have been offset for clarity.

contribution to $H_{1/2}$ in the $^4\mathbf{10}[\mathbf{56}^+]$ channel and large contribution in the $^2\mathbf{8}[\mathbf{70}^-]$ channel suggests that the helicity-1/2 data should lie below the global fit in the first resonance region and above the global fit at larger W. This is generally consistent with the data in Fig. 5.

The helicity-3/2 structure function is dominated in the resonance region by the Δ, with suppressed contributions in all other channels. Again this is consistent with the $H_{3/2}$ data being higher than the global fit in the Δ region and below the fit at larger W. The prediction of vanishing $H_{3/2}$ for the nucleon elastic contribution reflects the dominance of magnetic coupling assumed in the model [28], which is expected to be a better approximation at high

TABLE I: Relative strengths of $N \to N^*$ transitions for helicity structure functions $H_{1/2,3/2}$ in the SU(6) quark model [26]. The coefficients λ and ρ denote the relative strengths of the symmetric and antisymmetric contributions of the SU(6) ground state wave function, with the SU(6) limit corresponding to $\lambda = \rho$.

SU(6) rep.	$^2\mathbf{8}[\mathbf{56}^+]$	$^4\mathbf{10}[\mathbf{56}^+]$	$^2\mathbf{8}[\mathbf{70}^-]$	$^4\mathbf{8}[\mathbf{70}^-]$	$^2\mathbf{10}[\mathbf{70}^-]$	total
$H_{1/2}$	$9\rho^2$	$2\lambda^2$	$9\rho^2$	0	λ^2	$18\rho^2 + 3\lambda^2$
$H_{3/2}$	0	$6\lambda^2$	0	0	0	$6\lambda^2$

Q^2.

Summing over all channels, the ratio of helicity-3/2 to 1/2 structure functions is predicted to be $H_{3/2}/H_{1/2} = 2/7$, which coincides exactly with the quark-parton model results $u^-/u^+ = 1/5 = d^+/u^+$ and $d^-/d^+ = 2 = d^-/u^-$ for all x. These predictions are found to hold approximately at $x \sim 1/3$, but significant deviations are observed at larger x. Various scenarios for SU(6) symmetry breaking, consistent with quark-hadron duality, were considered in Ref. [27], leading to specific predictions for structure function ratios in the $x \to 1$ limit. The general trends of the duality violations persist even in the more realistic symmetry breaking scenarios, so that the deviations from unity in Fig. 5 can be understood, at least qualitatively, in terms of a microscopic quark-level description. Note also that the quark model predictions relate to the resonant components of the data *only*; the presence of the nonresonant background washes out these predictions somewhat, especially at larger Q^2, and its remarkable that the general trends of the duality violations in the various resonance regions nevertheless remain.

V. CONCLUSIONS

In this work we have performed the first detailed analysis of quark-hadron duality in individual $\gamma^* p$ helicity cross sections, utilizing recent data on inclusive unpolarized and polarized structure functions from Jefferson Lab. Unlike spin-dependent structure functions which can change sign as a function of x and Q^2, the helicity cross sections are by definition constrained to be positive definite. This reduces the dramatic violations of duality seen for

example in the proton g_1 structure function in the Δ resonance region, where the negative resonance contribution at low Q^2 makes way for a positive structure function in deep inelastic kinematics at large Q^2.

The data on the polarized and unpolarized structure functions are used to quantify the degree of duality violation in the helicity structure functions in each of the three prominent nucleon resonance regions, as well as over the entire range $W < 2$ GeV. We find that duality is realized more clearly for helicity-1/2 structure function $H_{1/2}$ than for the helicity-3/2 function $H_{3/2}$, with the duality violating corrections in the latter positive in the first resonance region and negative in the second resonance region. The duality violations are largest in the Δ region for both $H_{1/2}$ and $H_{3/2}$.

Over entire resonance region, the duality violating corrections are $\lesssim 10\%$ (and negative) for $H_{1/2}$ and $\lesssim 20\%$ (and positive) for $H_{3/2}$ at $Q^2 \leq 4$ GeV^2, which is rather smaller than the corresponding duality violation found in the spin-dependent g_1 structure function. The patterns of duality violation are in general agreement with expectations from quark models based on spin-flavor symmetry [26, 27].

Our results suggest that data above the Δ resonance region could be used to constrain *both* spin-averaged and spin-dependent parton distributions. This lends support to recent efforts to broaden the kinematic coverage in global fits of unpolarized PDFs [3] by lowering the Q^2 and W^2 cuts, and to extending these efforts to the polarized sector. Moreover, it raises the interesting possibility of performing global fits of helicity PDFs q^+ and q^- directly, rather than reconstructing these from separate unpolarized and polarized PDF analyses; such an enterprise would demand a consistent analysis of combined cross section and polarization asymmetry data along the lines presented in this work.

Acknowledgments

This work was supported by the U.S. Department of Energy under Contract No. DE-FG02-03ER41231, and DOE contract No. DE-AC05-06OR23177, under which Jefferson Science Associates, LLC operates Jefferson Lab.

[1] E. D. Bloom and F. J. Gilman, Phys. Rev. Lett. **25**, 1140 (1970).

[2] W. Melnitchouk, R. Ent and C. Keppel, Phys. Rept. **406**, 127 (2005).

[3] A. Accardi, M. E. Christy, C. E. Keppel, W. Melnitchouk, P. Monaghan, J. G. Morfín and J. F. Owens, Phys. Rev. D **81**, 034016 (2010).

[4] S. Alekhin, J. Blumlein, S. Klein and S. Moch, Phys. Rev. D **81**, 014032 (2010).

[5] I. Niculescu *et al.*, Phys. Rev. Lett. **85**, 1182, 1186 (2000).

[6] Y. Liang *et al.*, arXiv:nucl-ex/0410027.

[7] A. Psaker, W. Melnitchouk, M. E. Christy and C. Keppel, Phys. Rev. C **78**, 025206 (2008).

[8] S. P. Malace *et al.*, Phys. Rev. C **80**, 035207 (2009).

[9] P. E. Bosted *et al.*, Phys. Rev. C **75**, 035203 (2007).

[10] P. Solvignon *et al.*, Phys. Rev. Lett. **101**, 182502 (2008).

[11] T. Navasardyan *et al.*, Phys. Rev. Lett. **98**, 022001 (2007).

[12] Y. Kahn, W. Melnitchouk and S. Kulagin, Phys. Rev. C **79**, 035205 (2009).

[13] S. P. Malace, Y. Kahn, W. Melnitchouk and C. E. Keppel, Phys. Rev. Lett. **104**, 102001 (2010).

[14] S. J. Brodsky, arXiv:hep-ph/0006310.

[15] G. R. Farrar and D. R. Jackson, Phys. Rev. Lett. **35**, 1416 (1975).

[16] G. P. Lepage and S. J. Brodsky, Phys. Rev. D **22**, 2157 (1980).

[17] D. Drechsel, S. S. Kamalov and L. Tiator, Phys. Rev. D **63**, 114010 (2001).

[18] L. N. Hand, Phys. Rev. **129**, 1834 (1963).

[19] H. Avakian, S. J. Brodsky, A. Deur and F. Yuan, Phys. Rev. Lett. **99**, 082001 (2007).

[20] K. V. Dharmawardane *et al.*, Phys. Lett. B **641**, 11 (2006).

[21] M. E. Christy and P. E. Bosted, Phys. Rev. C **81**, 055213 (2010).

[22] S. Simula, M. Osipenko, G. Ricco and M. Taiuti, Phys. Rev. D **65**, 034017 (2002).

[23] J. Blumlein and H. Bottcher, Nucl. Phys. B **841**, 205 (2010).

[24] K. Abe *et al.*, Phys. Lett. B **452**, 194 (1999).

[25] S. Wandzura and F. Wilczek, Phys. Lett. B **72**, 195 (1977).

[26] F. E. Close and N. Isgur, Phys. Lett. B **509**, 81 (2001).

[27] F. E. Close and W. Melnitchouk, Phys. Rev. C **68**, 035210 (2003).

[28] F. E. Close, F. J. Gilman and I. Karliner, Phys. Rev. D **6**, 2533 (1972); F. E. Close and F. J. Gilman, Phys. Rev. D **7**, 2258 (1972); F. E. Close, H. Osborn and A. M. Thomson, Nucl. Phys. **B77**, 281 (1974).